Level 2 reliability of simplified pushover methods

L. Hermanns, M.O. González, E. Alarcón & A. Fraile
ETSII, Universidad Politécnica de Madrid, Spain.

J. Vega
CEMIM-F2I2,Madrid Spain.

SUMMARY:
Pushover methods are being used as an everyday tool in engineering practice and some of them have been included in Regulatory Codes. Recently several efforts have been done trying to look at them from a probabilistic viewpoint. In this paper the authors shall present a Level 2 approach based on a probabilistic definition of the characteristic points defining the response spectra as well as a probabilistic definition of the elasto-plastic pushover curve representing the structural behavior. Comparisons with Montecarlo simulations will help to precise the accuracy of the proposed approach.

Keywords: Reliability, Pushover, Level 2 method.

1. INTRODUCTION

Pushover methods have become common practice in seismic engineering. Their inclusion in Codes, their simplicity and the insight they provide are some of the reasons that explain their success. Practitioners and researchers can find a number of alternative methods in the literature aimed at different structural types and with variable complexities.

This paper explores the use of pushover methods in reliability analysis. More precisely, a level 2 approach will be used to estimate the failure probability of a structure under the action of seismic loads, with demand estimated by the pushover methodology proposed by Fajfar (Fajfar *et al.*1997 Fajfar 1999, Fajfar 2000, Dolsek & Fajfar 2007, Fajfar & Dolsek 2011). Randomness in the characteristics of both the action and the structure will be taken into account.

Although other factors can be selected, in order to show clearly the possibilities and limitation, a simple assumption has been made, i.e.: failure has been defined in terms of a limit global ductility (μ_{lim}). Thus the failure function $g(\underset{\sim}{x})$, which is dependent on the random variables of the problem, can be defined as:

$$g(\underset{\sim}{x}) = \mu_{lim} - \mu = 0; \quad \begin{cases} \mu < \mu_{lim}; \text{ Safety region} \\ \mu > \mu_{lim}; \text{ Failure region} \end{cases} \tag{1.1}$$

In the first part of this paper, the basic random variables will be assessed. Then, failure probabilities will be estimated using a level 2 approach. The values obtained will be compared with the equivalent ones considering Montecarlo simulations in order to assess the accuracy of the results. Finally, the weighting and sensitivity factors, which are byproducts of level 2 methods, will be discussed.

2. STATISTICAL CHARACTERIZATION OF THE RANDOM VARIABLES.

In this section, the basic random variables considered in the problem are presented and characterized. They are clustered in two groups: action variables, and structure variables.

2.1. Action random variables

2.1.1. Peak ground acceleration

Peak ground acceleration is the first random variable *a*. Lognormal distributions are often used to approximate the probability density function of the Peak Ground Acceleration (Baker and Cornell 2006). In this paper, the mean value has been obtained through a classical attenuation function (Mc Guire 1974), considering an epicentral distance R=20 km and a seismic event of magnitude M=8. Thus, the mean value is μ_a=0.6 g, and the coefficient of variation (CoV), consistent with the attenuation model, is CoV_a=0.55.

2.1.2. Plateau amplification factor and Transition Period

The second random variable is the relation between the value of the plateau in the response spectrum and the PGA. This variable will be named amplification factor A_f. Based on the works of Mohraz *et al.*(1973), the random variable is considered to distribute lognormally, with a mean value μ_{Af}=2.23, and standard deviation σ_{Af}=0.46.

The third random variable is the so-called transition period (Tc), which at the design spectrum sets the boundary between the plateau and the decay portion at higher periods.

The distribution of this random variable has been estimated based on a study using a set of 85 records selected from data bases covering a wide range of magnitudes and distances. For each record, a design spectrum displaying a plateau plus a decay portion inversely proportional to the vibration period has been obtained by minimization of squared differences. Each minimization produces a design spectrum, that is, a couple (A_f, Tc). Their cumulative distribution functions (CDF) are plotted in figure 1, together with the marginal lognoramal distributions that have been fitted to them. They indicate a CoV_{Tc}=40%, and a correlation between A_f and Tc $\rho_{Af\text{-}Tc}$=0.25. Those results have been retained, although the mean value has been assigned a slightly higher value (μ_{Tc}=0.6 s) in order to allow comparisons with results in Fajfar (2000).

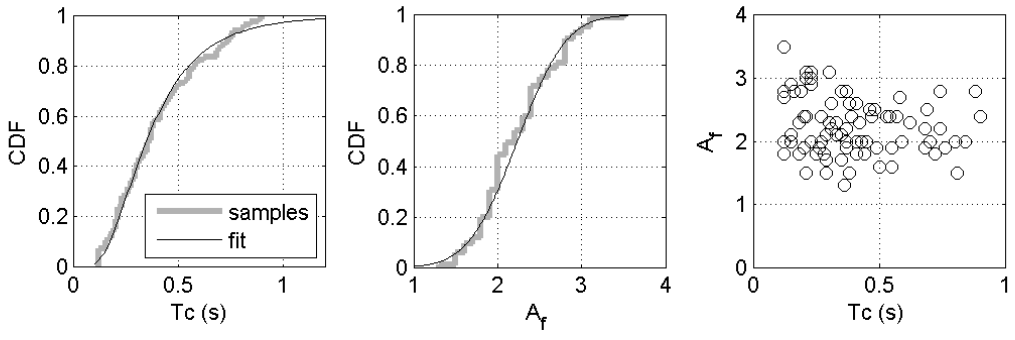

Figure 1. Joint characterization of A_f and Tc from 85 sample records.

2.2. Structure random variables

The fourth and fifth random variables relate to the structure. They are the normalized (according to the pushover procedure) force and displacement at yield (S_{ay^*}, D_{y^*}). They have been assigned mean values based on the desired global stiffness of the structure. In this work, two different structures have been considered: a stiffer one with μ_{Say^*}=0.39 g, μ_{Dy^*}=6.1 cm; and a more flexible one with the same μ_{Say^*} and μ_{Dy^*}=2.0 cm. Considering their mean values, the vibration periods for both structures are: 0.79 s

for the more flexible one (structure A), and 0.45 s for the stiffer one (structure B).

The form of the distributions and their standard deviations and correlation have been obtained based on a study on a structure taken from the litterature (Barbato *et al*. 2010). It is a three story, one bay 3D structure. A finite element (FE) model has been built using OpenSees (Mazzoni *et al*. 2007). Columns have been modelled using displacement-based Euler-Bernoulli frame elements with four integration points each. Their cross sections have been discretized in fibers of concrete and steel. Beams have been modelled using linear Euler-Bernoulli elements. Masses have been lumped at four points at each floor.

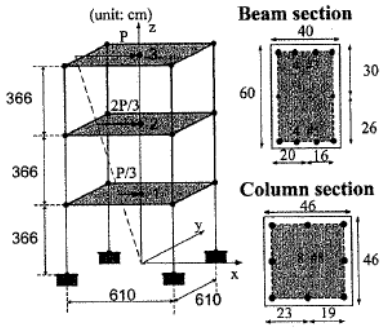

Figure 2. Structure used to assess the scatter of the capacity curve (Barbato et. al 2010)

Columns materials have been defined as follows. Concrete is modelled considering the Kent - Scott - Park concrete model. The strain at peak strength is set to be 0.2%, and the one at the ultimate strength is 0.5 %. Peak strength is characterized as a lognormal variable with mean value 35 MPa, and CoV=20%. The ultimate strength is 75% of the peak one. Steel is modelled as a bilinear material, with yield strength characterized also as a lognormal variable with mean value 300 MPa, and CoV=10%.

The random characteristics of the pushover curve have been estimated from a set of 150 sample pushover curves. Each sample structure has been built considering homogeneous characteristics in steel and concrete. From the set of 150 bilinearized push over curves it is possible to characterize the yield point as a set of two random variables: normalized yield force and normalized yield displacement. A good fit has been obtained considering their logarithms as jointly normal random variables. From this results, the random variables (normalized force and displacement at yield) have been supposed to distribute jointly as lognormal variables, with a CoV=0.05 in both cases and a correlation $\rho_{Say^*\text{-}Dy^*}$=0.90.

3. RESULTS

In this section failure probability considering the limit state defined in eq. 1.1 will be assessed for different values of the ductility limit. To this end a First Order Second Moment (FOSM) method will be used. FOSM methods approximate the limit state function by a linear equivalent at the design point. The accuracy of this approximation depends on the shape of the failure domain. The main benefit of FOSM methods, aside from being less time consuming, lies on two byproducts: the sensitivities of the reliability index and the weighting coefficients for an equivalent deterministic computation. These results provide additional insight into failure probability.

Failure probabilities computed using FOSM for a wide range of ductility limits, for both structures, will be presented next. In order to assess the accuracy of the results obtained using FOSM, a validation using Montecarlo simulation will be presented first.

3.1. Validation of FOSM results

Montecarlo method performs an estimation of failure probability based on the results obtained through a generally high number of samples. For each set of sampled basic variables, the ductility is computed, and then the set is clustered either among the safe set or among the unsafe one. If the number of samples is high enough, the failure probability can be assessed as the ratio between the number of elements in the unsafe set, and the total number of samples.

The validation of FOSM estimates has been done considering 1 million samples. Six test cases have been selected, resulting from the combination of structures A (more flexible) and B (stiffer), and three ductility limits (μ_{lim}=3, 4 y 6). Failure probabilities are presented in table 1. The values of failure probabilities using both methods are very similar. Therefore, it can be concluded that FOSM provides failure probability estimates that have a suitable accuracy for the problem at hand.

Pf %	Structure A		Structure B	
	Montecarlo	FOSM	Montecarlo	FOSM
μ_{lim}=3	29.12	29.67	55.30	57.30
μ_{lim}=4	16.77	17.14	39.13	40.27
μ_{lim}=6	6.13	6.29	19.95	20.13

Table 1. Failure probabilities as a function of the limit state and the assessment method.

3.2. Failure probability as a function of the ductility limit

FOSM has been applied to six different combinations of two structures (table 2) and three sets of variables defining the seismic action (table 3). Now, failure probabilities have been computed for a wide range of ductility limits. In addition to them, the weighting coefficients and sensitivity factors for all random variables have been estimated. These factors provide insight into the influence of each random variable at the design point.

Variable	Structure A	Structure B	Correlations
	Distribution: logN (μ, σ)		
S_{ay}^* (g)	logN (0.3899, 0.0195)		$\rho_{Say^*-Dy^*} = 0.90$
D_y^* (cm)	logN (6.1, 0.305)	logN (2.0, 0.100)	

Table 2. Statistical Characterization of basic random variables of the structure.

Variable	Action I	Action II	Action III	Correlations
	Distribution: logN (μ, σ)			
a (g)	logN (0.6, 0.33)	logN (0.4, 0.22)	logN (0.2, 0.11)	
Af (-)	logN (2.23, 0.46)			$\rho_{Af-Tc} = 0.25$
Tc (s)	logN (0.6, 0.24)			

Table 3. Statistical Characterization of basic random variables of the action.

Mean values in structural random variables lead to fundamental periods of vibration equal to 0.79 s (struct.A) and 0.45 s (struct.B). The application of the pushover procedure assigning mean values to all random variables leads to the ductility values listed in table 4.

	Structure A (T = 0.79 s)	Structure B (T = 0.45 s)
Action I (a = 0.6 g)	2.60	4.21
Action II (a = 0.4 g)	1.73	2.70
Action III (a = 0.2 g)	0.87	1.19

Table 4. Ductility values resulting from pushover method assigning mean values to all random variables.

Graphical representations of the pushover methodology, including both the response spectrum and the capacity curve, for the two cases relating action I are presented in figure 3. It is interesting to highlight that the intersections of the equivalent perfectly elastic capacity curves and the response spectrum lay at both sides of Tc.

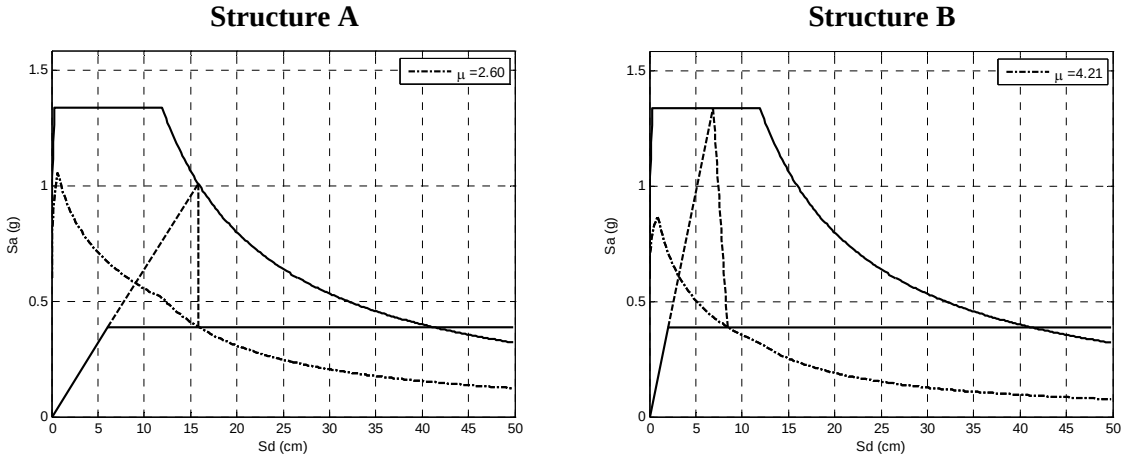

Figure 3. Design point obtained with the pushover methodology considering mean values of action I and structures A and B

The next figure displays the failure probability as a function of the ductility limit, for the six abovementioned combinations of the basic variables. In each case, ductility limits have been chosen above the ones listed in table 4, resulting from assigning mean values to all random variables. Thus, in all cases, the mean design point leads lays in the safe region. The reliability index β has also been plotted in figure 4. It measures the distance, in the space of uncorrelated and normalized basic random variables, between the origin and the design point.

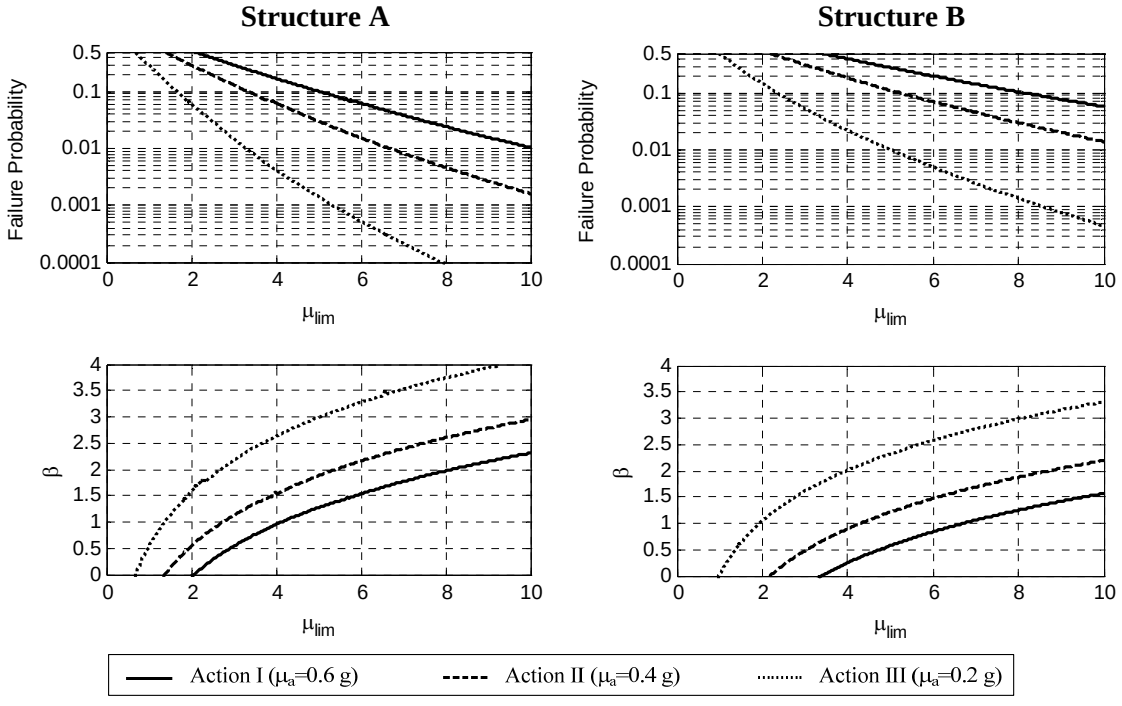

Figure 4. Failure probability and reliability index as a function of the ductility limit.

Results in figure 4 indicate that, for a given ductility limit, structure A displays lower failure probabilities than structure B, for all action characterizations. The reason is the comparatively higher

flexibility of structure A. For example, considering action III, failure probabilities below 1% are achieved when $\mu_{lim} > 3$ in structure A, while bigger values of ductility limit are needed ($\mu_{lim} > 5$) in the case of structure B.

A second, not surprising, conclusion is that a decrease in the mean value of the PGA leads to a global dwindling in failure probabilities. The two higher mean PGA values (0.4 and 0.6 g) lead to failure probabilities which are relatively higher. For example, if structure B and the highest value of ductility limit are considered, failure probability is above 1% for actions I and II, while it is lower than 0.1% for action III.

Figure 5 displays the, weighting coefficients (γ) and sensitivity factors (ξ) for all random variables, for the six abovementioned combinations of the basic variables.

The weighting coefficient is the ratio between the random variable value at the design point and its mean value. It allows clustering the random variables in two groups: load variables, if $\gamma > 1$; and resistance variables if $\gamma < 1$. All random variables associated to the seismic action act as loads, while the structure's variables act as resistences.

The higher weighting coefficients are associated with random variable a, followed by Tc. The random variables associated to the structure display weighting factors close to unity because of their reduced scatter. It is also interesting to point out that, for a given structure and ductility limit, weighting coefficients increase as the mean PGA value decreases. The reason is that the higher the PGA, the more likely it is to reach failure. Thus, the higher the mean PGA value, the more likely it is to have a design point close to it.

The same reasoning explains why structure A leads to higher weighting coefficients than structure B. For the same ductility limit, failure probabilities are lower with structure A, thus the design point is further from the mean values.

All plots in figure 5 display weighting coefficients which are equal to 1 at the lowest considered ductility limit. The range of ductility limits has been set so that its lowest vale is equal to the one in table 4. With this ductility limit, the failure surface intersects the origin of the space of uncorrelated normalized random variables.

The sensitivity factor indicates the influence of each random variable on failure probability close to the design point. Negative values indicate a decrease in failure probability as the random variable increases, while positive values are associated to increases in failure probabilities.

All random variables associated to the seismic action have negative normalized values, which are bigger in absolute value than the ones associated with the structure's random variables. Figure 5 display sensitivity factors which are not dependent on the structure nor the PGA level to a great extent. In addition to it, the dependence upon the ductility limit is very low in all cases.

The discontinuities in the sensitivity factors are associated with ductility limits where the design point is placed at the mean Tc value. This effect can be explained with reference to figure 6. Lower ductility limits lead to design points with the structure's fundamental period being higher than Tc (figure 6 (a)), while higher ductility limits the fundamental period is lower than Tc (figure 6 (b)).

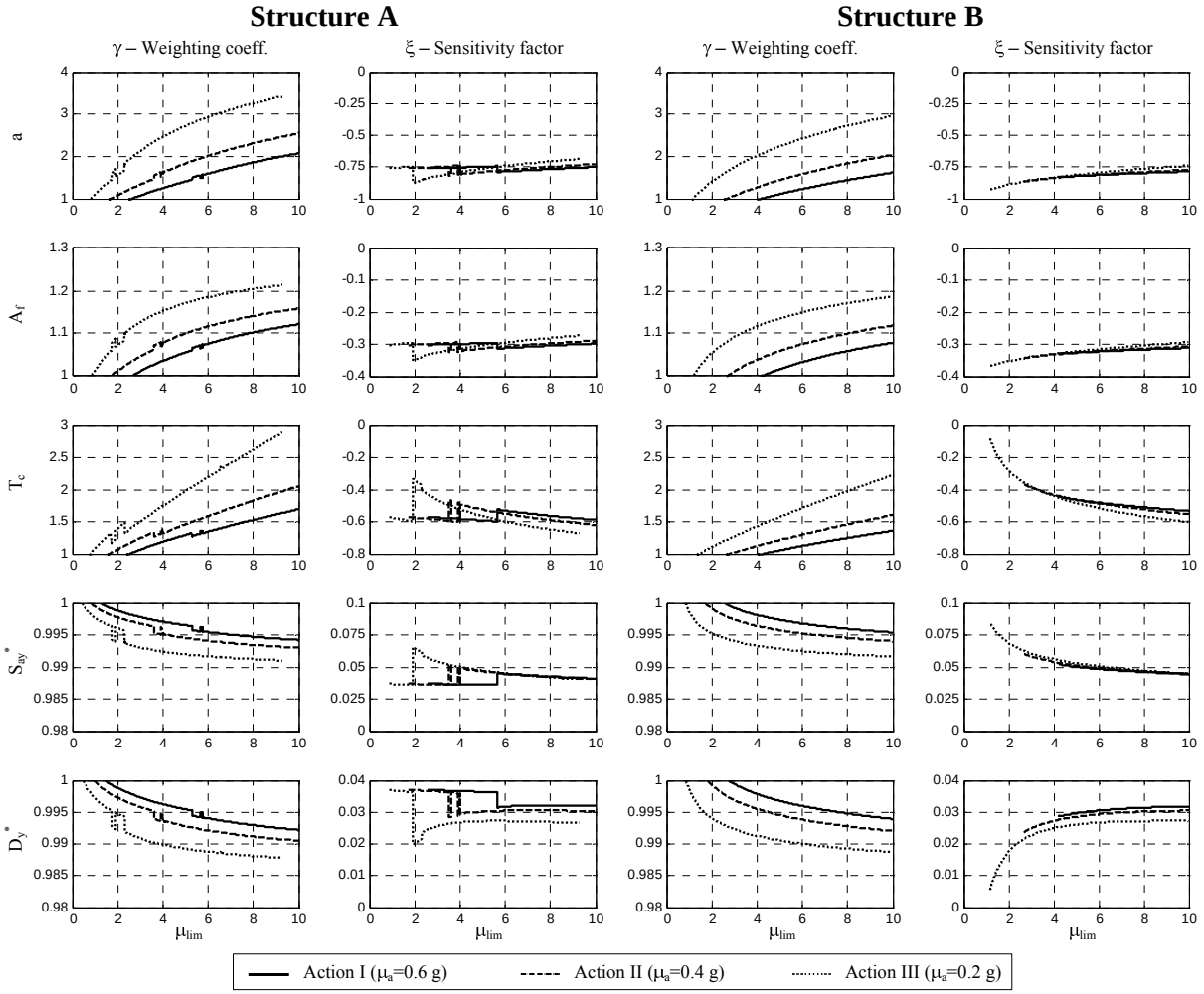

Figure 5. Weighting coefficients and sensitivity factors for all basic random variables.

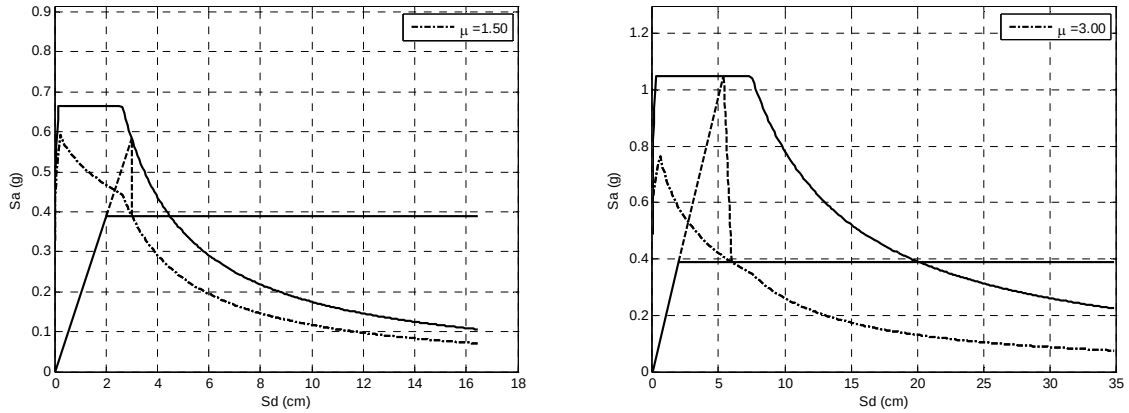

(a) (b)

Figure 6. Design point for action I and structure B, with ductility limits: (a) 1.50 and (b) 3.00

4. CONCLUSIONS

The use of pushover methods in seismic reliability analysis has been explored in this document. To this end two structures have been used, each of them characterized by two random variables. Randomness in the seismic action has been defined with a set of three variables.

First, the accuracy of FOSM methods has been assessed. For the case under study, FOSM methods have provided very good estimates of failure probabilities when compared with Montecarlo simulations, with relative errors in the range 1-4%.

Then, FOSM methods have been used to assess failure probabilities considering a wide range of global ductility limits. In addition to it, the weighting factors and sensitivity factors have provided more insight into failure probabilities. For example, it has been found that failure probabilities are more sensitive to action random variables than to structural ones, which seems to contradict recent results (Chen and Li 2010).

AKCNOWLEDGEMENT

M.O. González is recipient of a research fellowship sponsored by the Higher Education Department of the Dominican Republic.

REFERENCES

Baker, J. and Cornell, C.A. (2006). Correlation of Response Spectral Values for Multicomponent Ground Motions. *Bulletin of the Seismological Society of America.* **99: 1**, 1193-1217.

Barbato, M., Gu, Q. and Conte, J.P. (2010). Probabilistic Push-Over Analysis of Structural and Soil-Structure Systems. *Journal of Structural Engineering* **136:11**,1330-1341.

Chen, J. and Li, J. (2010). Stochastic seismic response analysis of structures exhibiting high nonlinearity. *Computers and Structures.* **88**, 395-412.

Dolsek, M., Fajfar, P. (2007). Simplified probabilistic seismic performance asessment of plan-asymmetric buildings. *Earthquake Engineering and Structural Dynamics.* **36: 13**, 2021-2041.

Fajfar, P., Gaspersic P., Drobnic, D. (1997). A simplified nonlinear method for seismic damage analysis of structures, in *Seismic design methodologies for the next generation of codes,* P. Fajfar and H. Krawinkler, Eds., Balkema, Rotterdam, 183-194.

Fajfar, P. (1999). Capacity spectrum method based on inelastic demand spectra. *Earthquake Engineering and Structural Dynamics.* **28: 9**, 979-993.

Fajfar, P. (2000). A Nonlinear Analysis Method for Performance Based Seismic Design. *Earthquake Spectra.* **16: 3**, 573-592.

Fajfar, P., Dolsek, M (2011). A practice-oriented estimation of the failure probability of building structures. *Earthquake Engineering and Structural Dynamics.* **41: 3**, 531-547.

Mazzoni, S., McKenna, F. and Fenves, G.L. (2007). OpenSees command language manual. Pacific Earthquake Engineering Research Center, Univ. of California at Berkeley. CA.

Mc Guire, R.K. (1974). Seismic Structural Response Risk analysis, Incorporation Peak Response Regression on Earthquake Magnitude and Distance, Dpt.Civ.Eng. Research Rep. R74-51, MIT.

Mohraz, B., Hall, W.J. and Newmark, N.M. (1973). A Study of Vertical and Horizontal Earthquake Spectra. *Report No. WASH-1255, prepared by Newmark Consulting Engineering Services for the Directorate of Licencing, US Atomic Energy Commision.*